PCCP

PAPER

View Article Online
View Journal | View Issue

Cite this: *Phys. Chem. Chem. Phys.*, 2016, **18**, 28797

Temperature dependence of acoustic vibrations of CdSe and CdSe–CdS core–shell nanocrystals measured by low-frequency Raman spectroscopy†

A. Jolene Mork, Elizabeth M. Y. Lee and William A. Tisdale*

Received 16th August 2016,
Accepted 3rd October 2016

DOI: 10.1039/c6cp05683k

www.rsc.org/pccp

We measure the temperature dependence of breathing-mode acoustic vibrations of semiconductor nanocrystals using low-frequency Raman spectroscopy. In CdSe core-only nanocrystals, the lowest-energy $\ell = 0$ mode red-shifts with increasing temperature by ~5% between 77–300 K. Changes to the interatomic bond distances in the inorganic crystal lattice, with corresponding changes to the bulk modulus and density of the material, contribute to the observed energy shift but do not fully explain its magnitude across all nanocrystal sizes. Invariance of the Raman linewidth over the same temperature range suggests that the acoustic breathing mode is inhomogeneously broadened. The acoustic phonons of CdSe/CdS core–shell composite nanocrystals display similar qualitative behavior. However, for large core–shell nanocrystals, we observe a higher-order Raman peak at approximately twice the energy of the $\ell = 0$ mode, which we identify as a higher spherical harmonic—the $n = 2$, $\ell = 0$ eigenmode—rather than a two-phonon scattering event.

1. Introduction

Semiconductor nanocrystals, commonly known as quantum dots (QDs), are highly tunable, quantum-confined materials with solid-state applications ranging from TVs to solar cells.[1,2] The myriad of applications of these materials stem from the small size of the semiconductor, where excited states are confined to occupy a finite volume and therefore allow only certain discrete energies, yielding a well-defined band-edge transition energy. The optical properties of QDs are not their only size-dependent feature, however; the acoustic phonons confined to the volume of a nanocrystal also exhibit highly size-dependent energies, with phonon frequency roughly inversely proportional to QD radius.[3] These acoustic phonons are known to play a role in QD thermalization,[4] exciton decoherence and dephasing,[5,6] and non-radiative relaxation processes,[7] among others. While several studies have examined how size[3] and polydispersity[8] play a role in the acoustic phonon energies, there has been little work targeted towards understanding how these phonon modes shift in energy as a function of temperature and what those dependencies reveal about the nature of the phonon modes themselves.

Temperature dependent frequency shifts and peak widths have been extensively studied for optical phonons in bulk crystals[9–11] and nanocrystals,[12–18] and are modeled using bond anharmonicity models. In particular, the longitudinal optical (LO) phonon has been shown to redshift in energy and broaden in linewidth with increasing temperature in CdSe nanocrystals,[12–18] but the temperature dependence of the acoustic phonons have received little attention. Results in ZnO nanocrystals at high temperatures (300–700 K) suggest that a simple anharmonic phonon–phonon decay mechanism cannot fully explain the observed temperature dependence of the energies and linewidths of acoustic phonon modes.[19] Temperature-dependent measurements of acoustic phonons in other nanocrystal materials systems are lacking, in spite of their relevance to low-temperature photoluminescence studies.[20–22]

Here we use low-frequency Raman spectroscopy to measure the temperature dependence of the acoustic phonons in several sizes of colloidally synthesized CdSe nanocrystals, as well as core–shell structures. Beyond the expected inverse size effect of the Raman-active acoustic phonons, the size- and temperature-dependent data reveal that changes to the crystal lattice of the inorganic core alone cannot fully explain the observed trends. Additionally, for CdSe/CdS core–shell nanocrystals, low-temperature Raman spectra reveal that higher order Raman features are the higher spherical harmonics of the fundamental breathing mode rather than multiphonon features.

2. Experimental details

2.1 Synthesis of colloidal nanocrystals

Colloidal QDs of various sizes were synthesized using a hot-injection method derived from Peng and Peng.[23] 120 mg of

Department of Chemical Engineering, Massachusetts Institute of Technology, Cambridge, MA, 02139, USA. E-mail: tisdale@mit.edu

† Electronic supplementary information (ESI) available. See DOI: 10.1039/c6cp05683k

CdO and 512 mg of *n*-octadecylphosphonic acid (ODPA) were added to 5.8 g of trioctylphosphine oxide (TOPO) in a 50 mL 3-neck round-bottom flask. These reagents were heated to 120 °C and degassed under vacuum for 1.5 hours, then heated to 300 °C under nitrogen until the brown suspension became a clear solution. At this point, 1.5 mL of trioctylphosphine (TOP) were injected into the flask, and the temperature was raised to 360 °C. When the solution reached this temperature, 0.9 mL of 1.7 M TOP–Se were swiftly injected into the flask with vigorous stirring. 1.5 mL aliquots were withdrawn from the reaction mixture approximately every 30 seconds after injection in order to obtain a size series of QDs. These aliquots were dissolved in 2 mL hexanes, and purified twice by precipitation with acetone and resuspension in hexanes. The resulting nanocrystals were stored in ambient conditions as a hexanes suspension before use.

2.2 Synthesis of core–shell nanocrystals

CdSe/CdS core–shell nanocrystals were synthesized according to Coropceanu and Bawendi,[24] with an initial wurtzite core of 1.6 nm in radius and a final radius after shell addition of 5.3 nm. Heteronanocrystals were purified by repeated precipitation with acetone and resuspension in hexanes. The purified nanocrystals were stored in hexanes under ambient conditions before use.

2.3 Low-temperature Raman spectroscopy

QD samples for Raman spectroscopy were drop cast from the stock solution to create optically dense thin films on single crystal quartz substrates. After drying in air, the samples were loaded into a ST-500 microscopy cryostat (Janis Research) and kept under vacuum for at least 12 hours before cooling with a cryogenic liquid (nitrogen or helium). Low-frequency non-resonant Raman spectra were acquired with a wavelength-stabilized 785 nm diode laser (Ondax), which, after passing several amplified spontaneous emission filters, reached the sample through a 40× 0.6 NA objective with a power density of about 1.8 mW μm^{-2}. Scattered light was collected in a back-scattering geometry, and Rayleigh-scattered light was filtered with two sequential notch filters (Ondax) which, combined, resulted in eight orders of magnitude Rayleigh suppression. Raman spectra were imaged using a 0.5 m focal length spectrograph with 1200 g mm^{-1} dispersion grating and a Peltier-cooled CCD camera (Princeton Instruments). The overall resolution of the instrument was 0.44 cm^{-1}. Each spectrum represents the average of three spectra acquired for 90 seconds. At least five minutes elapsed between measurements at different temperatures in order to ensure temperature stabilization before each measurement.

3. Results and discussion

3.1 CdSe core-only QDs

In order to understand how the acoustic phonon energies of QDs vary as a function of temperature, we synthesized a series of colloidal QDs according to Peng and Peng,[23] where aliquots were removed at various reaction times in order to achieve an array of sizes. These aliquots were purified by precipitation,

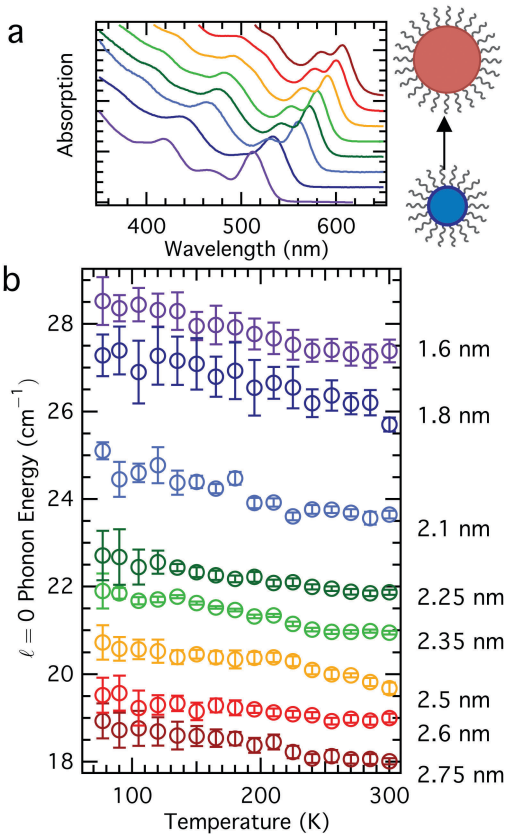

Fig. 1 Phonon mode softening in QD nanocrystals. (a) Absorption spectra and illustration of the CdSe QD samples used in this study. (b) Temperature dependence of acoustic phonon energy for several sizes of CdSe QD cores with core diameter indicated along right side of panel. Individual QD samples are color-coordinated across both panels.

and all samples were treated the same in order to minimize sample-to-sample differences that might result from, for example, different ligand coverage on different QD samples.[25,26] The Raman spectra of these samples all reveal the same trend: a phonon mode softening (redshift) with increasing temperature (Fig. 1) without concomitant change in the phonon linewidth (Fig. 2). For LO phonons in nanocrystals, the phonon linewidth is typically decomposed into a temperature-dependent contribution and a temperature independent contribution, resulting from an intrinsic zone-center phonon linewidth derived from its lifetime and a phonon-confinement effect broadening, respectively.[12] Acoustic phonons, unlike optical phonons, have no linewidth contribution from the sampling of a larger region of the Brillioun zone due to the phonon confinement effect; rather, their homogeneous linewidth results from their lifetime and damping with the environment. The nanoparticles studied showed no consistent change in linewidth as a function of temperature, and in general had nearly temperature independent linewidth, within the error of the measurement (Fig. 2b). This suggests that inhomogenous contributions to the linewidth from, for example, many different sizes of QDs (QD sample had polydispersity $\leq$10%) or strong environmental damping, dominate contributions to the acoustic phonon linewidth in these materials. As can be seen in Fig. 2b,

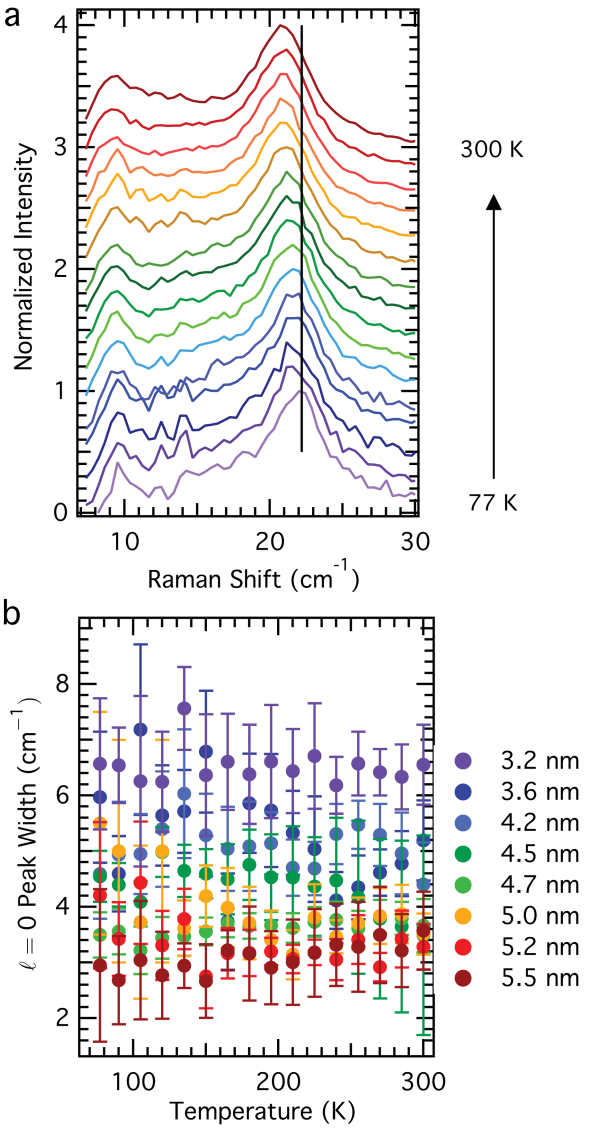

Fig. 2 Temperature-invariance of Raman linewidth. (a) Low-frequency Raman spectra for D = 4.7 nm diameter CdSe QDs at temperatures in 15 K increments between 77 K and 300 K, where the black vertical line centered for the low-temperature peak serves as a guide to the eye. (b) The Raman linewidth is invariant with sample temperature for all sizes studied (QD core diameter indicated to the right of the panel). Error bars represent the 95% confidence interval for the fitted linewidth.

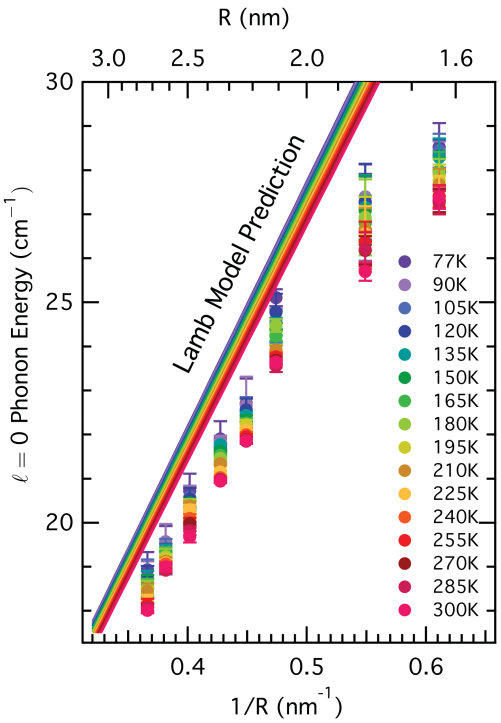

Fig. 3 Measured temperature dependence deviates from theoretical predictions. Acoustic phonon energy as a function of inverse QD size (1/radius) for temperatures between 77 K and 300 K (dots) and the Lamb model prediction for the same temperature range (lines).

the linewidth in general decreases with increasing particle size, consistent with predictions based on environmental damping.[27,28] However, this same trend can also be explained by sample polydispersity; QD batches having smaller average diameter tend to have greater size dispersity.[29]

Acoustic phonon modes in CdSe QDs have been frequently understood using the elastic sphere model, first described by Lamb,[30] which yields phonon energies inversely proportional to the QD size. Though the modes with angular momentum number ℓ = 0 and ℓ = 2 are known to be Raman active,[31] this study focuses on the ℓ = 0 mode for more facile interpretation. The equations governing the vibrations of an elastic sphere are sensitive not only to the size of the material, but also its elastic properties, given by its bulk modulus or transverse and longitudinal sound velocities, and its density. For CdSe, both of these are known to change with temperature: the bulk modulus changes by less than 5% over the temperature range between 77–300 K,[32] while the density changes by less than 1% in this range.[33] Incorporating these known changes in the physical properties of the CdSe core results in some expected variation in the nanoparticle acoustic phonon frequencies as a function of temperature, but it is insufficient to fully explain the observed trends. In Fig. 3, we compare the temperature-dependent Raman spectra as a function of QD size to the predictions based on Lamb's model after accounting for changes in the bulk modulus and density at various temperatures. The Lamb model consistently over-predicts phonon frequency for a particular size, yet under-predicts the observed variation in phonon frequency for all sizes of nanocrystals over the measured temperature range. The smallest nanocrystals exhibit the greatest deviation from Lamb model calculations both in the absolute value of the phonon energy as well as the temperature-dependent variation ($\sim$2 cm^{-1} observed variation, compared to 1 cm^{-1} predicted), suggesting that other factors beyond those traditionally considered in the Lamb model may play a role in defining acoustic phonon frequencies in colloidal nanocrystal films.

We hypothesize that the QD ligands, organic molecules with a significantly different elastic modulus bound to the nanocrystal surface, may play an important role in determining acoustic phonon frequencies in these materials.[26] While other models have considered the effect of an elastic medium on the linewidth and acoustic phonon damping,[34] these organic ligands

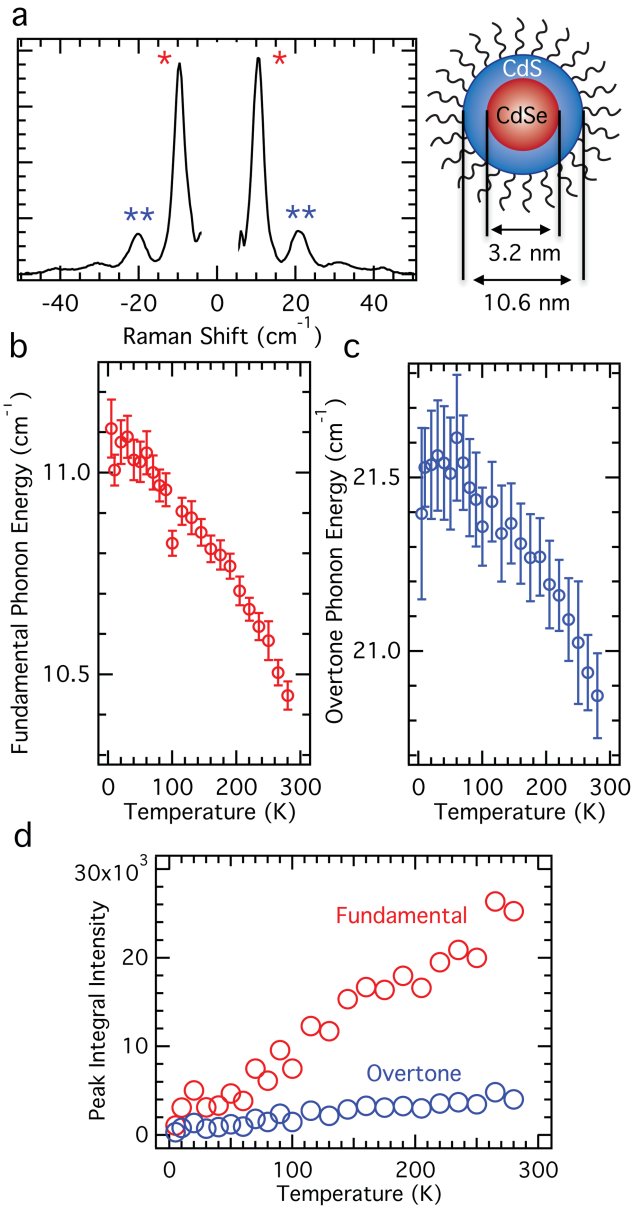

Fig. 4 Acoustic phonons in spherical core–shell nanocrystals. (a) Low-frequency Raman spectrum of CdSe/CdS core–shell nanocrystals having 3.2 nm diameter CdSe core and 3.7 nm thick CdS shell. The fundamental phonon peak is marked as ω_1 and the second feature is marked ω_2. Two more higher-order phonon modes are visible in this spectrum collected at 300 K. (b) Peak center energy for the fundamental acoustic phonon mode as a function of temperature. (c) Peak center energy for the overtone phonon mode as a function of temperature. (d) Integrated peak intensities for the fundamental (red) and overtone (blue) phonons between 4 K and 300 K.

have not been explicitly modeled (in part because many studies of acoustic phonons in nanocrystals have focused exclusively on those embedded into glasses). Especially for small nanocrystals, where the surface-to-volume ratio is high and the total core mass is low, the inertial mass of the ligands may significantly affect the vibrational energies sustained within the inorganic core.[26,35] While the Lamb model for vibrating elastic spheres predicts much of the variation in eigenmode frequency with particle size, it alone does not fully capture the temperature-dependent behavior of the acoustic modes in nanocrystals and highlights the necessity for models that explicitly account for surface ligands.

3.2 CdSe–CdS core–shell QDs

In addition to core-only nanocrystals, we also report on the temperature-dependent behavior of acoustic phonons in the more technologically-relevant core–shell nanostructures. Room temperature Raman spectra of the thick shell CdSe/CdS nanocrystals reveal the fundamental $\ell = 0$ Raman mode (labelled ω_1), as well as a series of higher order modes at higher energies, of which the first is labelled ω_2 in Fig. 4a. These phonon features display a similar temperature-dependent redshift in energy as was observed for core-only nanocrystals (Fig. 4b and c), demonstrating again that any model for nanocrystal phonon mode energies must account for sample temperature. Also like the core-only CdSe QDs, the Raman linewidth of the phonon mode shows no variation with sample temperature within the error of the measurement. These data imply that the same fundamental physics govern both core-only and core–shell nanocrystals in the low-temperature regime.

Temperature-dependent Raman spectroscopy reveals the identity of the higher order mode, ω_2, allowing discrimination between a two-phonon Raman scattering process and a single eigenmode with approximately twice the energy of the $\ell = 0$ fundamental mode (*i.e.* the $n = 2$ spheroidal mode). The temperature dependent intensities for the fundamental and second harmonic peaks are plotted between 4 K and 300 K in Fig. 4d. The nearly linear temperature dependence of the ω_2 mode characterizes a one-phonon process; a two-phonon Raman scattering process would yield a quadratic dependence on temperature.[36] Additionally, from Fig. 4b and c, the temperature dependent energy shift is approximately equivalent for both the ω_1 and ω_2 modes, while a two-phonon process would have resulted in a $2\times$ larger energy shift with temperature for the second harmonic. From these data, we confidently assign the ω_2 mode to single-phonon Raman scattering from the $n = 2$ eigenmode, as has been observed for silver nanoparticles.[37] Other higher order phonon modes are observed in Fig. 4a with energies close to $3\omega_1$ and $4\omega_1$, but these features could not be conclusively assigned due to weak low-temperature signal.

4. Conclusions

We collected Raman spectra of CdSe and CdSe/CdS core–shell QDs between cryogenic temperatures and room temperature and monitored the response of the acoustic phonon Raman features. All samples studied exhibited a temperature-dependent mode softening at higher temperatures, consistent with expected changes in the bulk elastic properties and density of the core material, but the magnitude of the temperature-dependent shift suggests that changes to the environment surrounding the inorganic nanocrystal, including the organic surface ligands, may also play a role in determining the QD phonon energies. The negligible change in Raman linewidth over the temperature range studied in both types of nanocrystals likely results from

inhomogeneous broadening (for example, due to polydispersity) that greatly exceeds any temperature-dependent change to the homogeneous linewidth derived from the phonon lifetime. Finally, we resolve for the first time the $n = 2$, $\ell = 0$ acoustic phonon mode for large CdSe/CdS core–shell nanoparticles.

Acknowledgements

This work was supported by Eni S.p.A. under the Eni-MIT Solar Frontiers Center.

Notes and references

1 K. Bourzac, *Nature*, 2013, **493**, 283.
2 P. V. Kamat, *J. Phys. Chem. C*, 2008, 18737–18753.
3 L. Saviot, B. Champagnon, E. Duval, I. A. Kudriavtsev and A. I. Ekimov, *J. Non-Cryst. Solids*, 1996, **197**, 238–246.
4 D. Hannah, N. Dunn, S. Ithurria, D. Talapin, L. Chen, M. Pelton, G. Schatz and R. Schaller, *Phys. Rev. Lett.*, 2011, **107**, 13–16.
5 S. Dong, D. Trivedi, S. Chakrabortty, T. Kobayashi, Y. Chan, O. V. Prezhdo and Z. H. Loh, *Nano Lett.*, 2015, **15**, 6875–6882.
6 A. P. Alivisatos, *J. Phys. Chem.*, 1996, **100**, 13226–13239.
7 D. Bozyigit, N. Yazdani, M. Yarema, O. Yarema, W. M. M. Lin, S. Volk, K. Vuttivorakulchai, M. Luisier, F. Juranyi and V. Wood, *Nature*, 2016, **531**, 618–622.
8 M. Ivanda, K. Furić, S. Musić, M. Ristić, M. Gotić, D. Ristić, A. M. Tonejc, I. Djerdj, M. Mattarelli, M. Montagna, F. Rossi, M. Ferrari, A. Chiasera, Y. Jestin, G. C. Righini, W. Kiefer and R. R. Gonçalves, *J. Raman Spectrosc.*, 2007, **38**, 647–659.
9 T. Hart, R. Aggarwal and B. Lax, *Phys. Rev. B: Solid State*, 1970, **1**, 638–642.
10 J. Menendez and M. Cardona, *Phys. Rev. B: Condens. Matter Mater. Phys.*, 1984, **29**, 2051.
11 M. Liu, L. Bursill, S. Prawer and R. Beserman, *Phys. Rev. B: Condens. Matter Mater. Phys.*, 2000, **61**, 3391–3395.
12 A. Tanaka, S. Onari and T. Arai, *Phys. Rev. B: Condens. Matter Mater. Phys.*, 1992, **45**, 6587.
13 N. G. Guo, Z. F. Zhou, Y. L. Huang, X. X. Yang, R. Jiang, Z. S. Ma and C. Q. Sun, *Chem. Phys. Lett.*, 2013, **585**, 167–170.
14 P. Kusch, H. Lange, M. Artemyev and C. Thomsen, *Solid State Commun.*, 2011, **151**, 67–70.
15 K. R. Zhu, M. S. Zhang, Q. Chen and Z. Yin, *Phys. Lett. A*, 2005, **340**, 220–227.
16 X. X. Yang, Z. F. Zhou, Y. Wang, R. Jiang, W. T. Zheng and C. Q. Sun, *J. Appl. Phys.*, 2012, **112**, 83508.
17 X. Fu, H. An and W. Du, *Mater. Lett.*, 2005, **59**, 1484–1490.
18 P. Mishra and K. Jain, *Phys. Rev. B: Condens. Matter Mater. Phys.*, 2000, **62**, 14790–14795.
19 H. K. Yadav, K. Sreenivas, R. S. Katiyar and V. Gupta, *J. Raman Spectrosc.*, 2011, **42**, 1620–1625.
20 M. J. Fernee, B. N. Littleton, S. Cooper, H. Rubinsztein-Dunlop, D. E. Gómez and P. Mulvaney, *J. Phys. Chem. C*, 2008, **112**, 1878–1884.
21 D. Oron, A. Aharoni, C. de Mello Donega, J. van Rijssel, A. Meijerink and U. Banin, *Phys. Rev. Lett.*, 2009, **102**, 1–4.
22 P. Borri, W. Langbein, S. Schneider, U. Woggon, R. L. Sellin, D. Ouyang and D. Bimberg, *Phys. Rev. Lett.*, 2001, **87**, 157401.
23 Z. A. Peng and X. Peng, *J. Am. Chem. Soc.*, 2001, **123**, 183–184.
24 I. Coropceanu and M. G. Bawendi, *Nano Lett.*, 2014, **14**, 4097–4101.
25 V. M. Dzhagan, I. Lokteva, M. Y. Valakh, O. E. Raevska, J. Kolny-Olesiak and D. R. T. Zahn, *J. Appl. Phys.*, 2009, **106**, 84318.
26 A. Girard, L. Saviot, S. Pedetti, M. D. Tessier, J. Margueritat, H. Gehan, B. Mahler, B. Dubertret and A. Mermet, *Nanoscale*, 2016, **8**, 13251–13256.
27 M. Montagna and R. Dusi, *Phys. Rev. B: Condens. Matter Mater. Phys.*, 1995, **52**, 10080–10089.
28 P. Verma, W. Cordts, G. Irmer and J. Monecke, *Phys. Rev. B: Condens. Matter Mater. Phys.*, 1999, **60**, 5778–5785.
29 J. R. Caram, H. Zheng, P. D. Dahlberg, B. S. Rolczynski, G. B. Griffin, D. S. Dolzhnikov, D. V. Talapin and G. S. Engel, *J. Chem. Phys.*, 2014, **140**, 84701.
30 H. Lamb, *Proc. London Math. Soc.*, 1882, **13**, 189–211.
31 E. Duval, *Phys. Rev. B: Condens. Matter Mater. Phys.*, 1992, **46**, 5795–5797.
32 B. Bonello and B. Fernandez, *J. Phys. Chem. Solids*, 1993, **54**, 209–212.
33 H. Iwanaga, A. Kunishige and S. Takeuchi, *J. Mater. Sci.*, 2000, **35**, 2451–2454.
34 S. K. Gupta, P. K. Jha and a. K. Arora, *J. Appl. Phys.*, 2008, **103**, 124307.
35 G. Cerullo, S. De Silvestri and U. Banin, *Phys. Rev. B: Condens. Matter Mater. Phys.*, 1999, **60**, 1928–1932.
36 P. M. A. Sherwood, *Vibrational Spectroscopy of Solids*, Cambridge University Press, 1972.
37 A. Nelet, A. Crut, A. Arbouet, N. Del Fatti, F. Vallée, H. Portalès, L. Saviot and E. Duval, *Appl. Surf. Sci.*, 2004, **226**, 209–215.